

Supplementary Material

A novel anti-hyperglycemic sulfated pyruvylated polysaccharide from marine macroalga *Hydropuntia edulis*

Anjaly Thambi^{1,2}, Kajal Chakraborty^{*1}

Central Marine Fisheries Research Institute, Ernakulam North P.O., P.B. No. 1603, Cochin 682018, Kerala, India

Short title: Anti-hyperglycemic pyruvylated polysaccharide from *Hydropuntia edulis*

***Corresponding author.** Marine Bioprospecting Section of Marine Biotechnology, Fish Nutrition and Health Division, Central Marine Fisheries Research Institute, Ernakulam North, P.B. No. 1603, Cochin 682018, Kerala, India

Tel.: +91 484 2394867, fax: +91 484 2394909

E-mail address: kajal_cmfri@yahoo.com (K. Chakraborty)

¹Marine Biotechnology, Fish Nutrition and Health Division, Central Marine Fisheries Research Institute, Ernakulam North, P.B. No. 1603, Cochin 682018, Kerala, India

²Department of Applied Chemistry, Cochin University of Science and Technology, Cochin, Kerala State, India

Funding and acknowledgements

The authors gratefully acknowledge the funding by the Indian Council of Agricultural Research (ICAR, New Delhi, India) (grant ID MBT/HM/SUB/23). The authors thank the Director, ICAR-Central Marine Fisheries Research Institute (ICAR-CMFRI), and Head, Marine Biotechnology, Fish Nutrition and Health Division, ICAR-CMFRI for facilitating the research. The authors are thankful to the Head, Department of Applied Chemistry, Cochin University of Science and Technology (Kerala State, India) for necessary support. A.T. gratefully acknowledges the Council of Scientific and Industrial Research for financial support.

Abstract

Dipeptidyl peptidase is a crucial enzyme that regulates glucose metabolism by degrading incretins, such as glucagon-like-peptide-1, thereby reducing insulin secretion from the pancreatic β -cells. Consequently, dipeptidyl peptidase-IV inhibitors are important remedial approach to moderate the hyperglycemic pathophysiology. A pyruvylated polysaccharide characterized as $[\rightarrow 3)\text{-}4,6\text{-}O\text{-}(1\text{-carboxyethylidene})\text{-}\beta\text{-D-galp}\text{-}(2\text{SO}_3^-)\text{-}(1\rightarrow 4)\text{-}3,6\text{-}\alpha\text{-L-AnGalp}\text{-}(2\text{OMe})\text{-}(1\rightarrow)]$, isolated from the marine macroalga *Hydropuntia edulis*, showed attenuation potential against dipeptidyl peptidase-IV (IC_{50} 4.44 μM). The structure was elucidated using mass and one/two-dimensional nuclear magnetic resonance spectroscopic analyses of hydrolyzed polysaccharide besides glycosidic linkages obtained from partially methylated alditol acetate derivative. The isolated polysaccharide also revealed potential anti-carbolytic properties against α -amylase/ α -glucosidase (IC_{50} 45-47 μM). The results proved the candidacy of pyruvylated polysaccharide isolated from *H. edulis* as a potential therapeutic lead against hyperglycemia.

Keywords: Marine macroalga *Hydropuntia edulis*; pyruvylated polysaccharide; anti-hyperglycemic activity; dipeptidyl peptidase-IV inhibitor

Supplementary material

Supplementary material S1. Identification of algae and accession number

Supplementary material S2. Chemicals, reagents, and instrumentation

Supplementary material S3. Analytical methods

Supplementary material S4. Deproteination of crude polysaccharide

Supplementary material S5. Chemical methods

Table S1. Percentage yield and bioactivities of crude polysaccharide of red marine macroalgae belonging to the subclass Rhodophyta

Table S2. Chemical composition of purified polysaccharide fractions from the aqueous extract of *H. edulis*

Table S3. Assignment of IR bands in SP-He-2

Table S4. ¹H and ¹³C NMR chemical shifts of residue of SP-He-2

Table S5. The binding energy, docking score, inhibition constant, intermolecular energy and torsional free energy between SP- He-2 motif and the active site of DPP-IV.

Figure S1. Elution profile of SP-He-2

Figure S2. Monosaccharide composition analysis of SP-He-2 and standards

Figure S3. HR-ESIMS spectrum of SP-He-2

Figure S4. UV-visible spectrum of SP-He-2

Figure S5. Infra-red spectrum of SP-He-2

Figure S6. ¹H NMR spectrum of hydrolyzed SP-He-2

Figure S7. ¹³C NMR spectrum of hydrolyzed SP-He-2

Figure S8. DEPT¹³⁵ spectrum of hydrolyzed SP-He-2

Figure S9. ¹H-¹H COSY NMR spectrum of hydrolyzed SP-He-2

Figure S10. HSQC spectrum of hydrolyzed SP-He-2

Figure S11. EI-MS spectrum of 3-*O*-acetyl-2,4,6-tri-*O*-methyl galactitol

Figure S12. EI-MS spectrum of 4-*O*-acetyl-3,6-anhydro-2-*O*-methyl galactitol

Figure S13. Lineweaver-Burk plots for the inhibition of SP-He-2 on DPP-IV

Figure S14. Molecular docking analysis of SP-He-2 and hydrogen bonds of polysaccharide unit

Supplementary material S1 Identification of algae and accession number

The algae sample of *G. corticata* was compared with that listed as item number (8) of the phylum Rhodophyta (red algae) as “*Gracilaria corticata* var. *corticata* J.Agardh, 1852, Gracilariaceae AC.3.1.1.2” (at page number 40 of Marine Biodiversity Museum, Catalogue 2018). Please read the citation as “Joshi KK et al (2018) Marine Biodiversity Museum, Catalogue 2018. CMFRI Special Publication No. 129, 140 p. ISSN 0972-2351”.

The algae sample of *H. edulis* was compared with that listed as item number (11) of the phylum Rhodophyta (red algae) as “*Gracilaria edulis* P. Silva, 1952, Gracilariaceae AC.3.1.1.5” (at page number 40 of Marine Biodiversity Museum, Catalogue 2018). Please read the citation as “Joshi KK et al (2018) Marine Biodiversity Museum, Catalogue 2018. CMFRI Special Publication No. 129, 140 p. ISSN 0972-2351”.



CATALOGUE-2018

Marine Biodiversity Museum

CATALOGUE-2018
Marine Biodiversity Museum

CMFRI Special Publication No.129
January 2018

Published by
Dr. A. Gopalakrishnan

Director
ICAR- Central Marine Fisheries Research Institute
P. B. 1603, Ernakulam North P. O., Kochi – 682 018, Kerala, India
E-mail: director@cmfri.org.in

Authors
K. K. Joshi, K.S. Sobhana, Molly Varghese, Miriam Paul Sreeram, K. R. Sreenath, P.M Geetha, K. M. Sreekumar, Aju K. Raju, M. S. Varsha, M. Sethulakshmi, K.A.Divya, Thobias P. Antony, K. B. Sheeba and A. Gopalakrishnan

Photography
P. R. Abhilash

Design
Blackboard

Publication production & Co- ordination
Library and Documentation Centre

ICAR- Central Marine Fisheries Research Institute
Post Box No. 1603, Ernakulam North P.O., Kochi-682 018.
Phone: +91 484 2394357, 2394867 Fax: +91 484 2394909
E-mail: contact@cmfri.org.in
www.cmfri.org.in

ISSN 0972-2351
© CMFRI 2018 All rights reserved. Material contained in this publication may not be reproduced in any form without the permission of the publisher

Citation: K. K. Joshi, K.S. Sobhana, Molly Varghese, Miriam Paul Sreeram, K. R. Sreenath, P.M Geetha, K. M. Sreekumar, Aju K. Raju, M. S. Varsha, M. Sethulakshmi, K.A.Divya, Thobias P. Antony, K. B. Sheeba and A. Gopalakrishnan. 2018. Catalogue- 2018. Marine Biodiversity Museum, CMFRI Special Publication No. 129, 140 p

PHYLUM RHODOPHYTA			
1	<i>Centroceras clavulatum</i> (C.Ag.) Montagne, 1846	Ceramiaceae	AC.8.1.1.1
2	<i>Spyridia fusiformis</i> Borgesen, 1937	Ceramiaceae	AC.8.1.2.1
3	<i>Champia globulifera</i> Borgesen, 1937	Champiaceae	AC.7.1.1.1
4	<i>Cheilosporum spectabile</i> Harvey ex Grunow, 1874	Corallinaceae	AC.5.1.2.1
5	<i>Jania rubens</i> (Linn.) Lamouroux, 1816	Corallinaceae	AC.5.1.3.1
6	<i>Gelidiella acerosa</i> (Forssk.) Feldmann & G. Hamel, 1934	Gelidiellaceae	AC.2.1.1.1
7	<i>Gracilaria arcuata</i> Zanardini, 1858	Gracilariaceae	AC.3.1.1.1
8	<i>Gracilaria corticata</i> var. <i>corticata</i> J.Agardh, 1852	Gracilariaceae	AC.3.1.1.2
9	<i>Gracilaria corticata</i> var. <i>pudumadamensis</i> V. Krishnamurthy & Rajendran, 1987	Gracilariaceae	AC.3.1.1.3
10	<i>Gracilaria salicornia</i> (C.Ag.) Dawson, 1954	Gracilariaceae	AC.3.1.1.4
11	<i>Gracilaria edulis</i> P. Silva, 1952	Gracilariaceae	AC.3.1.1.5

40 | Marine Biodiversity Museum, Catalogue 2018

The algal sample of *Gracilaria corticata* var. *corticata* J. Agardh, 1852 (Gracilariaceae) (voucher number AC.3.1.1.2) (listed as item number 8, at page number 40 of Marine Biodiversity Museum, Catalogue 2018). The algal sample of *Gracilaria edulis* P. Silva, 1952 (Gracilariaceae) (syn-*Hydropuntia edulis* Gurgel & Fredericq 2004) (voucher number AC.3.1.1.5) (listed as item number 11, at page number 40 of Marine Biodiversity Museum, Catalogue 2018). The algal sample of *P. hornemanii* was compared with that listed as item number (26) of the phylum Rhodophyta (red algae) as “*Portieria hornemanii* (Lyngbye) P.C.Silva, 1987, Rhizophyllidaceae (voucher number AC.4.2.1.1)” (at page number 41 of Marine Biodiversity Museum, Catalogue 2018). Please read the citation as “Joshi KK et al (2018) Marine Biodiversity Museum, Catalogue 2018. CMFRI Special Publication No. 129, 140 p. ISSN 0972-2351”. The algal sample of *A. spicifera* was compared with that listed as item number (28) of the phylum Rhodophyta (red algae) as “*Acanthophora spicifera* (Vahl.) Borgesen, 1910, Rhodomelaceae (voucher number AC.8.2.1.2)” (at page number 41 of Marine Biodiversity Museum, Catalogue 2018). Please read the citation as “Joshi KK et al (2018) Marine Biodiversity Museum, Catalogue 2018. CMFRI Special Publication No. 129, 140 p. ISSN 0972-2351”.

26	<i>Portieria homemannii</i> (Lyngbye) P.C.Silva, 1987	Rhizophyllidaceae	AC.4.2.1.1
27	<i>Acanthophora muscoides</i> (Linn.) Bory de Saint-Vincent, 1828	Rhodomelaceae	AC.8.2.1.1
28	<i>Acanthophora spicifera</i> (Vahl.) Borgesen, 1910	Rhodomelaceae	AC.8.2.1.2
29	<i>Chondria cornuta</i> Borgesen, 1932	Rhodomelaceae	AC.8.2.3.1
30	<i>Laurencia papillosa</i> (C.Ag.) Greville, 1830	Rhodomelaceae	AC.8.2.2.1
31	<i>Laurencia poitei</i> (Lam.) M.A.Howe, 1918	Rhodomelaceae	AC.8.2.2.2
32	<i>Botryocladia leptopoda</i> (J.Ag.) Kylin, 1931	Rhodymeniaceae	AC.7.2.1.1
33	<i>Scinaia bengalica</i> Borgesen, 1938	Scinaiaceae	AC.1.1.1.1
34	<i>Kappaphycus alvarezii</i> (Doty) ex P.C.Silva, 1996	Solieriaceae	AC.6.2.1.1
35	<i>Sarconema filiforme</i> (Sonder) Kylin, 1932	Solieriaceae	AC.6.2.2.1
36	<i>Solieria robusta</i> (Grev.) Kylin, 1934	Solieriaceae	AC.6.2.3.1

Supplementary material S2. Chemicals, reagents, and instrumentation

Previously reported methods were adopted for formulating buffers and molar solutions requisite for various assays. Varian Cary 50 ultra-violet-visible (UV-VIS) spectrophotometer was utilized for recording spectrophotometry of samples. Infra-red (IR) spectra were recorded using KBr pellets within a scan range of 4000 and 400 cm^{-1} by utilizing Perkin-Elmer Series 400 FTIR spectrophotometer equipped with an air-cooled deuterated triglycine sulfate (DTGS) detector and results were expressed in % transmittance with a resolution of 4 cm^{-1} . Nuclear magnetic resonance (NMR) spectra (one and two dimensional) of purified polysaccharide were recorded at Bruker AVANCE III spectrometer operating at 500 MHz (AV 500) (Bruker, Karlsruhe, Germany) using deuterated water (D_2O) as solvent and tetramethylsilane (TMS) as the internal standard. ^1H , ^{13}C , and $^{135}\text{DEPT}$ NMR spectra were recorded at 512, 12000 and 6000 scans, respectively, while ^1H - ^1H -COSY and HSQC experiments were performed at 8 and 16 scans, respectively. Obtained results were processed using MestReNova (version 7.1.1-9649, Mestrelab Research S.L) software. Analytical high performance liquid chromatography (HPLC) (Shimadzu Corporation, Nakagyo-ku, Japan) equipped with an elusive light scattering diode (ELSD) detector connected to an amino column (Luna 250 \times 4.6 mm, 5 μm) (Phenomenex, USA) was employed for identifying monosaccharide composition of purified polysaccharide fraction. Electron impact (EI) ionization method was utilized for performing gas chromatography mass spectrometric (GC-MS) analysis operated at 70 eV (Perkin-Elmer Clarus-680, Winter Street, Waltham, MA, USA), and derivatised polysaccharide sample was fractionated using SPB[®]-1 Supelco, USA, capillary column. Helium was used as the carrier gas at a flow rate of 0.9 mL min^{-1} . HRESIMS (high-resolution electrospray ionization) spectra were recorded in electron spray ionization with negative mode by employing a mass spectrometer (Agilent 6520 Q-TOF LC/MS/MS, Santa Clara, CA) combined with a high-pressure liquid chromatography (HPLC) fitted with a reverse phase octadecylsilane bonded (C_{18}) column (1.8 μm , 2.1 mm \times 5 cm).

Supplementary material S3. Analytical methods

Screening of antioxidant activity

Antioxidant inhibition potentials were evaluated by 2,2'-azino-bis-3-ethylbenzothiazoline-6- sulfonic acid (ABTS^+) and 1,1-diphenyl-2-picryl-hydrazil (DPPH) radical assays. Different sample concentrations (125-2000 ppm) were mixed with freshly prepared DPPH solution (1 mL) in methanol (80 $\mu\text{g/mL}$) before being incubating under dark at room temperature for 30 min. The reduction in absorbance of the mixture was recorded at 517 nm. To assess the ABTS scavenging activity, ABTS (7 μM) dissolved in distilled water was mixed with potassium persulfate (2.45 μM) before being incubated in dark at room temperature for 16 hours. ABTS^+ stock solution was diluted with methanol to document an absorbance of 0.70 at 734 nm. Diluted ABTS^+ solution (3 mL) was mixed with the test samples (30 μL), and the absorbance was noted after 6 min at 734 nm. The results were indicated as IC_{50} (median inhibition concentration) values, which were obtained from the graph laid with sample concentration vis-à-vis percentage inhibition by enzymes/radicals in μM . Similarly, hydrogen peroxide and metal ion chelating assay were done according to the procedure reported by Yang et al., 2008.

Thiobarbituric acid reactive species (TBARS) inhibitory activity

TBARS assay utilizes the ability of crude polysaccharides to inhibit lipid peroxidation. Previously reported method by Kulisic et al., 2004 was adopted for performing experiment wherein lipid source was lyophilized green mussel (*Perna viridis*). At 532 nm absorbance was measured spectrophotometrically and results were expressed as mM of MDA equivalent compounds formed per kg sample (MDAEQ/kg sample).

Screening of anti-hyperglycemic activity

Anti-hyperglycemic properties of the studied compounds were evaluated by using serine protease DPP-4 and carbohydrate hydrolyzing α -amylase/ α -glucosidase enzyme attenuating potential (Antony, Chakraborty, & Dhara, 2022; Krishnan, Chakraborty, & Dhara, 2021). For DPP-4 enzyme inhibition assay, test samples (0.35 mL; 125, 250, 500, 1000, 2000 ppm) and aliquot of DPP-4 in 0.1 M tris-HCl (pH 8) buffer (0.05 U/mL enzyme, 0.05 M, pH 7.5, 15 μ L) were mixed before being incubated at 37 °C (for 30 min) together with gly-pro-p-nitroanilide (0.05 mL, 0.2 M in tris HCl buffer). The reaction was terminated with glacial acetic acid (25%, 0.025 mL), and the absorbance was recorded at 405 nm. To analyze α -glucosidase inhibition, the test samples (0.5 mL; 125, 250, 500, 1000, 2000 ppm) and aliquot of α -glucosidase in tris-HCl buffer (1 U/mL enzyme, 0.2 M, pH 8, 0.5 mL) were mixed before being incubated at 37 °C (for about 5 min). The reaction mixture was added with starch solution (2% w/v; 0.5 mL) and incubated at 35 °C (for 15 min). The reaction was terminated with dinitrosalicylic acid (1 mL) in a boiling water bath before being cooled and diluted with distilled water (9 mL). The absorbance of the reaction mixture was measured at 540 nm. To analyze α -amylase inhibition, various concentrations (as above) of test samples (0.5 mL) and aliquot of α -amylase (0.5 mg/mL) in phosphate buffer (1 U/mL enzyme, 0.2 M, pH 6.9, 0.5 mL) were mixed before incubating at 25 °C (for about 10 min). The reaction mixture was added with starch solution (1% w/v; 0.5 mL in 0.02 M sodium phosphate buffer, pH 6.9) and incubated at 25 °C (for 10 min). The reaction was terminated with dinitrosalicylic acid (1 mL) in a boiling water bath before being cooled and diluted with distilled water (9 mL). The absorbance of the reaction mixture was measured at 540 nm.

Screening of anti-inflammatory activity

Anti-inflammatory activity of crude polysaccharides was performed using 5-lipoxygenase (5-LOX), cyclooxygenase-1 (COX-1) and cyclooxygenase-2 (COX-2) enzyme as done in previously reported procedure (Larsen, Dahl, Bremer, 1996; Baylac, & Racine, 2003). For 5-LOX, samples were analyzed via the addition of algal extracts in phosphate buffer (0.1 M, pH 9.0) to the enzyme (0.1 mL) before the start of reaction followed by the addition of linoleic acid (10 μ L). Absorbance was measured for the samples at 234 nm on a 96 well plate reader. The basic protocol for the COX-1/2 assays are the same. 10 μ L of the COX-1/2 enzyme and 50 μ L of the co-factor solution (0.003 g L-adrenalin and 0.003 g reduced glutathione in 10 mL 0.1 M Tris buffer, pH 8.2) were pre-incubated for 15 min on ice. This solution (60 μ L) was added to the test solution (2.5 μ L algal extract + 17.5 μ L water) and pre-incubated for 5 min at room temperature. Arachidonic acid

(20 μ L) was added to this enzyme-extract mixture and incubated exactly for 8 min in a water bath at 37 °C. The reaction was terminated with 10 μ L 2N HCl. Absorbance was recorded at 587 nm.

Supplementary material S4. Deproteination of crude polysaccharide

Crude polysaccharide from *H. edulis* (SP-He) was subjected to deproteination as previously reported by Staub, (1965). Initially, Sevag reagent (chloroform: *n*-butanol, 5:1, v/v) was mixed with polysaccharide sample and stirred for 30 min. The content was centrifuged to collect upper layer, and again treated with Sevag reagent (x 5) until white layer disappears. The solution was analyzed using UV spectrophotometer at 260 nm and 280 nm to ensure that it is free of proteins followed by removal of Sevag reagent and precipitation using ethanol. After centrifugation at 2000 rpm for 20 min, the precipitate was collected and washed several times using petroleum ether, acetone and ethanol, before being lyophilized. The yield of the polysaccharide has been calculated as $\{(\text{weight of polysaccharide}/\text{weight of dried algal mass}) \times 100\}$.

Supplementary material S5. Chemical methods

Total carbohydrate

Total carbohydrate determination of polysaccharide fractions was done according to the method of Dubois et al., 1956 using glucose as standard. 1 mL of the polysaccharide samples were prepared in distilled water ranging from 0-100 μ g/mL and 1 mL of 5 % phenol solution was added to it. This was followed by addition of 5 mL concentrated sulfuric acid, mixed well and incubated for 10 minutes at room temperature. A blank (distilled water) was recorded to zero using spectrophotometer and absorbance of samples was measured at 488 nm. A graph was plotted using absorbance of glucose samples against its known concentrations. A linear regression was attained with a correlation factor of $R^2 = 0.9961$ and an equation of $y = 0.003x + 0.112$. This equation was further utilized for calculating total carbohydrate in the polysaccharide. Total carbohydrate (%) = $\{(X) (V) (100)/ (W) (10^6)\}$, where X = concentration of sample obtained from the graph equation, V = total volume of solution (7 mL), W = weight of polysaccharide (in grams).

Total uronic acid

Initially, polysaccharide samples were prepared in various concentrations ranging from 0-100 μ g/mL in distilled water. 0.1 mL of sample was then carefully layered on to a test tube containing 6 mL of ice-cold sulfuric acid. This is mixed well with constant cooling. It is then heated in a water bath at 100 °C for 10 minutes and again cooled to room temperature. This is followed by addition of 0.2 mL of 0.1 % alcoholic solution of carbazole. Then the solution is mixed again, heated at 55 °C for 30 minutes and cooled to room temperature. Absorbance was measured at 530 nm using distilled water as the blank. A graph was plotted using absorbance of glucuronic acid against its known concentrations. A line formula $y = 0.040x + 0.183$ was further obtained from the graph. Total uronic acid content (%) = $\{(X)(V)(100)/ (W)(10^6)\}$, where X =

concentration of sample obtained from graph equation, V = total volume of solution (6.3 mL), W = weight of polysaccharide (in grams).

Total sulfate content

Sulfate content of polysaccharide samples was determined by turbidimetric procedure reported by Dodgson et al., 1962 using K₂SO₄ (potassium sulfate) (100-100 µg/mL) solution. A standard curve was plotted to obtain a linear equation, $y = 0.15x + 0.00$. For determining the sulfate content, initially, the sample (4 mg) was hydrolyzed using 2 mL of 2 N HCl by heating it at 60-75 °C for 6 hours. To the 0.2 mL of the hydrolyzed sample, 3.8 mL 3 % trichloroacetic acid (TCA), 1mL gelatin-barium chloride was added, mixed thoroughly and incubated at room temperature for 20 minutes. At 360 nm absorbance was measured using 2 N HCl as blank. Total sulfate content (%) = $\{(X)(V)(100)/ (W)(10^6)\}$, where X = concentration of sample obtained from graph equation, V = total volume of solution (5 mL), W = weight of polysaccharide (in grams).

Total protein content

Protein quantification was done by Lowry's method according to procedure used by Lowry et al., 1951 utilizing bovine serum albumin (BSA) as standard. Standard calibration curve was plotted by measuring absorbance of BSA with different concentration. To 0.1 g of polysaccharide sample in an eppendorf, 1 mL distilled water, 1 mL TCA was added and shaken well. Centrifugation at 1000 rpm at 4 °C for 20 minutes yielded supernatant which was then treated with 5 mL of reagent I (48 mL of 2 % Na₂CO₃ in 0.1 N NaOH, 1 mL 0.5 % CuSO₄. 5 H₂O) and incubated for 10 minutes at room temperature. This was followed by addition of 0.5 mL of freshly prepared reagent II (Folin-ciocalteau reagent:H₂O, 1:1) and again incubated for 30 minutes at room temperature. At 660 nm, absorbance of sample was measured spectrophotometrically and the unknown concentration was calculated from standard curve equation, $y = 0.0012 + 0.1699$. Total protein content (%) = $\{(X)(V) (100)/ (W) (10^6)\}$, where X = concentration of the sample obtained from graph equation, V = total volume of solution (6.5 mL), W = weight of polysaccharide (in grams).

Pyruvic acid

Pyruvic acid content was examined by following procedure reported by Koepsell et al., 1952 utilizing pyruvic acid as the standard. A standard calibration curve was plotted by taking absorbance of pyruvic acid in different concentrations (10-60 µg/mL). Pyruvic acid content of polysaccharide of *H. edulis* was evaluated by dissolving sample (5 mg) in 1mL of 0.02 M oxalic acid. This was followed by hydrolyzing sample at 120 °C for 3 hours, mixed it well before opening and then cooled to room temperature. 0.5 mL of hydrolyzed polysaccharide was then dissolved in 1 mL of 0.75 M sulfuric acid and mixed well. To this 0.5 mL of 2,4-dinitrophenylhydrazine hydrochloric acid solution was added and kept at room temperature for 20 minutes. In order to eliminate side products, solution was separated using ethyl acetate (5 mL) and upper layer was

collected. Again 3 mL of 10 % sodium carbonate solution was added, lower layer was collected and absorbance was recorded at 380 nm against distilled water as blank.

References

- Antony T, Chakraborty K, Dhara S. 2022. Sulfated galactofucan from seaweed *Padina tetrastromatica* attenuates proteolytic enzyme dipeptidyl-peptidase-4: A potential anti-hyperglycemic lead. *Nat Prod Res.* E-Pub ahead of print, 1–12. 10.1080/14786419.2022.2025802.
- Baylac S, Racine P. 2003. Inhibition of 5-lipoxygenase by essential oils and other natural fragrant extracts. *Int J Aromather.* 13:138–42. [https://doi.org/10.1016/S0962-4562\(03\)00083-3](https://doi.org/10.1016/S0962-4562(03)00083-3).
- Dodgson K, Price R. 1962. A Note on the determination of the ester sulfate content of sulfated polysaccharides. *Biochem J.* 84:106–110. 10.1042/bj0840106.
- Dubois M, Gilles KA, Hamilton JK, Rebers PT, Smith F. 1956. Colorimetric method for determination of sugars and related substances. *Anal Chem.* 28(3):350–356. doi: 10.1021/ac60111a017.
- Koepsell HJ, Sharpe ES. 1952. Microdetermination of pyruvic and α -ketoglutaric acids, *Arch Biochem Biophys.* 38(1):443–449. doi: 10.1016/0003-9861(52)90050-7.
- Krishnan S, Chakraborty K, Dhara S. 2021. Biomedical potential of β -chitosan from cuttlebone of cephalopods. *Carbohydr Polym.* 273:118591. 10.1016/j.carbpol.2021.118591.
- Kulisic T, Radonic A, Katalinic V, Milos M. 2004. Use of different methods for testing antioxidative activity of oregano essential oil. *Food Chem.* 85:633–40. <https://doi.org/10.1016/j.foodchem.2003.07.024>.
- Larsen LN, Dahl E, Bremer J. 1996. Peroxidative oxidation of leucodichlorofluorescein by prostaglandin H synthase in prostaglandin biosynthesis from polyunsaturated fatty acids. *Biochim Biophys Acta.* 1:47–53. 10.1016/0005-2760(95)00188-3.
- Lowry OH, Rosebrough NJ, Farr AL. 1951. Randall RJ, Protein measurement with the Folin phenol reagent. *J Biol Chem.* 193:265–275. PMID: 14907713.
- Staub A. 1965. Removal of protein-Sevag method. *Methods in Carbohydrate Chemistry*, 5:5–6.
- Yang B, Zhao M, Shi J, Yang N, Jiang Y. 2008. Effect of ultrasonic treatment on the recovery and DPPH radical scavenging activity of polysaccharides from Longan fruit pericarp. *Food Chem.* 106:685–690. <https://doi.org/10.1016/j.foodchem.2007.06.031>.

Table S1. Percentage yield and bioactivities of crude polysaccharide of red marine macroalgae belonging to the subclass Rhodymeniophycidae

	<i>G. corticata</i>	<i>P. hornemannii</i>	<i>A. spicifera</i>	<i>H. edulis</i>
Yield [§]	4.90 ± 0.05	1.20 ± 0.75	2.80 ± 0.88	5.10 ± 0.56
TBARS activity ^ε	0.97 ^c ± 0.08	2.85 ^a ± 0.88	1.70 ^b ± 0.89	0.72 ^d ± 0.96
Anti-oxidant activity[†]				
DPPH scavenging	0.49 ^c ± 0.56	0.85 ^a ± 0.87	0.65 ^b ± 0.03	0.32 ^d ± 0.32
ABTS scavenging	0.36 ^c ± 0.58	0.82 ^a ± 0.06	0.58 ^b ± 0.32	0.21 ^d ± 0.68
H ₂ O ₂ scavenging	0.30 ^c ± 0.30	0.71 ^a ± 0.08	0.52 ^b ± 0.16	0.25 ^c ± 0.02
Fe ₂ ⁺ scavenging	0.31 ^c ± 0.02	0.75 ^a ± 0.22	0.59 ^b ± 0.50	0.29 ^c ± 0.16
Anti-inflammatory activity[†]				
5-LOX inhibitory	0.63 ^c ± 0.02	1.79 ^a ± 0.59	0.71 ^b ± 0.25	0.52 ^d ± 0.52
COX-1 inhibitory	0.82 ^c ± 0.22	1.5 ^a ± 0.62	0.85 ^b ± 0.12	0.75 ^d ± 0.06
COX-2 inhibitory	0.70 ^b ± 0.21	1.21 ^a ± 0.65	0.72 ^b ± 0.2	0.61 ^c ± 0.72
Anti-hyperglycemic activity[†]				
DPP-IV inhibitory	0.31 ^c ± 0.76	0.71 ^a ± 0.08	0.62 ^b ± 0.06	0.21 ^d ± 0.05
α-amylase inhibitory	0.47 ^c ± 0.25	0.95 ^a ± 0.05	0.59 ^b ± 1.75	0.31 ^d ± 0.83
α-glucosidase inhibitory	0.32 ^b ± 0.76	0.75 ^a ± 0.59	0.72 ^a ± 0.49	0.26 ^c ± 0.04
Anti-hypertensive activity[†]				
ACE-I inhibition	0.91 ^c ± 0.07	1.21 ^a ± 0.03	1.01 ^b ± 0.87	0.87 ^c ± 0.08
Anti-hypercholesterolemic activity				
HMGCR inhibition	0.81 ^c ± 0.25	1.03 ^a ± 0.95	0.9 ^b ± 0.56	0.75 ^d ± 0.02

[§]Yield as % w/w.

^εTBARS activity was represented as mM MDAEQ kg⁻¹.

[†]Bioactivities were expressed as IC₅₀ values (mg/mL). The samples were analyzed in triplicate (n = 3) and expressed as mean ± standard deviation. Means followed by different superscripts (a-d) within the same row indicated significant differences (*p* < 0.05).

Table S2. Chemical composition of purified polysaccharide fractions from the aqueous extract of *H. edulis*

Fractions	SP-He [§]	SP-He-1 [‡]	SP-He-2 [‡]	SP-He-3 [‡]	SP-He-4 [‡]	Standard
Yield [†]	4.90 ^a ± 0.07	14.50 ^c ± 0.57	32.50 ^b ± 0.08	19.80 ^d ± 0.77	14.30 ^c ± 0.09	-
Chemical composition of purified fractions[†]						
Carbohydrate	55.20 ^a ± 0.62	19.10 ^c ± 0.71	65.60 ^b ± 0.58	26.20 ^d ± 0.38	30.67 ^c ± 0.07	-
Protein [©]	5.36 ^a ± 0.05	nd	1.38 ^b ± 0.32	0.04 ^c ± 0.55	nd	-
Sulfate [€]	8.5 ^a ± 0.98	1.12 ^c ± 0.41	2.36 ^b ± 0.25	0.9 ^d ± 0.27	0.19 ^c ± 0.11	-
Uronic acid [¥]	2.00 ^a ± 0.26	9.43 ^c ± 0.27	0.97 ^b ± 0.01	2.19 ^d ± 0.32	1.97 ^c ± 0.58	-
Pyruvic acid [£]	9.07 ^a ± 0.26	0.07 ^c ± 0.87	15.4 ^b ± 0.71	1.3 ^d ± 0.52	nd	-
Monosaccharide composition^{††}						
Gal	62.5	42	58	43.5	36	-
AnGal	35	28	40	23.6	18	-
Xyl	2	6	nd	3	nd	-
Mann	nd	nd	nd	nd	nd	-
Glc	nd	4	nd	5.5	nd	-
Anti-hyperglycemic activity[†]						
DPP-IV inhibition	4.65 ^e ± 0.12	10.32 ^b ± 0.78	4.44 ^c ± 0.51	18.89 ^a ± 0.66	17.87 ^a ± 0.21	4.21 ^c ± 0.01 ^A
α -amylase inhibition	48.26 ^a ± 0.09	60.29 ^c ± 0.52	45.25 ^b ± 0.48	75.96 ^d ± 0.85	72.98 ^c ± 0.07	50.56 ^d ± 0.25 ^B
α -glucosidase inhibition	49.32 ^a ± 0.07	61.97 ^c ± 0.16	47.02 ^b ± 0.15	77.05 ^d ± 0.11	73.15 ^c ± 0.15	50.15 ^d ± 0.02 ^B

[†]The yield and chemical composition were expressed as % w/w.

The chemical composition analyses were carried out in triplicate (n = 3) and were expressed as mean ± standard deviation.

Means followed by different superscripts (a-e) within the same row indicated significant differences ($p < 0.05$).

[§]SP-He is the ethyl alcohol precipitate and freeze-dried aqueous polysaccharide concentrate of *H. edulis*

[‡]SP-He-1 through SP-He-4 are the column fractions eluted with increasing concentrations of 0.1-0.4 M NaCl gradient.

[§]Total carbohydrate content (% w/w) = $\{(A) \times B/C\}$, where A = concentration of the polysaccharide fraction obtained from graph, B = total volume of solution taken, and C = weight of the polysaccharide

[©]Protein concentration was determined with Folin phenol reagent, and expressed as % w/w of polysaccharide fraction

[€]Total sulfate content was determined by turbidimetric method, and the absorbance of the test solution was recorded at 360 nm against blank reading. Standard curve was developed with K₂SO₄ solution and sulfate content (% w/w) of polysaccharide fraction was calculated from standard curve.

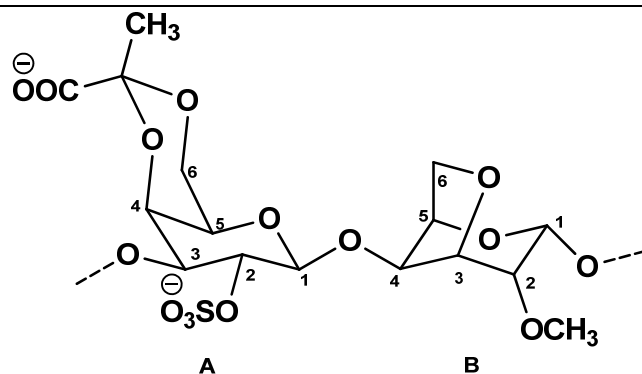
[¥]Uronic acid content was estimated by carbazole method, and was calculated by (%w/w) = $\{(A) \times B/C\}$, where A = concentration of the polysaccharide fraction obtained from graph, B = total volume of solution and C = weight of polysaccharide in mg

[£]Pyruvic acid content was examined by utilizing 2,4-dinitrophenylhydrazine hydrochloric acid solution and pyruvic acid as the standard.

^{††}Monosaccharide compositions of the fractions were expressed as mol %. nd signifies 'not detected'. Bioactivity was expressed as IC₅₀ values (μ M). Letters A-B indicate standards used: A- diprotein-A, B- acarbose

Table S3. Assignment of IR bands in SP-He-2

Wavenumber (cm⁻¹)	Assignment
3462.76	-OH stretching vibrations
2930.57	-CH stretching vibrations
1620.60	Carboxylate anion of the pyruvate moiety
1447.01	C-C-H vibrations
1339.57	Presence of sulfate esters
1261.20	C-C and C-O stretching in pyranoid ring, C-O-C stretching of glycosidic bonds
1143.07	C-O of pyranosyl ring
1077.01	Skeletal mode of galactans
1030.67	C-O and C-C stretching of pyranose ring
930.22	Vibration of C-O-C bridge, characteristic of 3,6-anhydrogalactose
830.47	2-O-sulfate group in D-galactose, secondary equatorial sulfate of the 1,3-linked galactose unit
746.14	Skeletal bending of galactose
687.18	Skeletal bending of galactose

Table S4. ^1H and ^{13}C NMR chemical shifts of residue of SP-He-2

Residue	C. No.	^{13}C NMR	^1H NMR	COSY
β -D-galactose linked to 3,6- α -L-anhydrogalactose	A1	96.5	4.48 (d, $J = 8.2$ Hz)	H-A2
	A2	72.8	3.74	H-A3
	A3	71.7	3.55	H-A4
	A4	72.9	3.39	-
	A5	73.3	3.58	-
	A6	68.4	3.80	H-A5
	Methyl	27.9	1.99	-
	Acetal	100.4	-	-
Carboxyl	177.4	-	-	
3,6- α -L-anhydrogalactose linked to β -D-galactose	B1	92.3	5.15 (d, $J = 2.8$ Hz)	H-B2
	B2	72.1	3.49	-
	B3	82.6	3.86	-
	B4	77.6	4.55	-
	B5	77.9	4.59	-
	B6	68.6	3.73	-
B2-Methyl	58.5	3.30	-	

^aNMR spectra were recorded using a Bruker AVANCE III 500 MHz (AV 500) spectrometer (Bruker, Karlsruhe, Germany).

^aValues were denoted in ppm. Multiplicity and coupling constants ($J = \text{Hz}$) were indicated in parentheses. Multiplicities were allocated by $^{135}\text{DEPT}$ NMR spectrum.

The assignments were made with the aid of the ^1H - ^1H COSY, ^1H - ^{13}C HSQC/HMBC and NOESY experiments.

Table S5. The binding energy, docking score, inhibition constant, intermolecular energy and torsional free energy between SP- He-1 motif and the active site of DPP-IV.

†Ligand	‡Binding energy (Kcal mol⁻¹)	‡Docking score (Kcal mol⁻¹)	‡Inhibition constant Ki (nM)	‡Intermolecular energy (Kcal mol⁻¹)	‡ Torsional free energy (Kcal mol⁻¹)	Hydrogen bonded residues	Distance from hydrogen bonded residue (Å)
SP-He-2	-1.76	-0.25	5.57	-3.24	+0.30	Ser ^{239.A} , Ser ^{239.B} , Tyr ^{241.B} , Phe ^{713.A}	2.662, 2.551, 2.929, 2.463, 3.189

†Molecular docking simulations were carried out using Autodock 4 software tool.

‡Values were evaluated from the calculations based on the energy minimization.

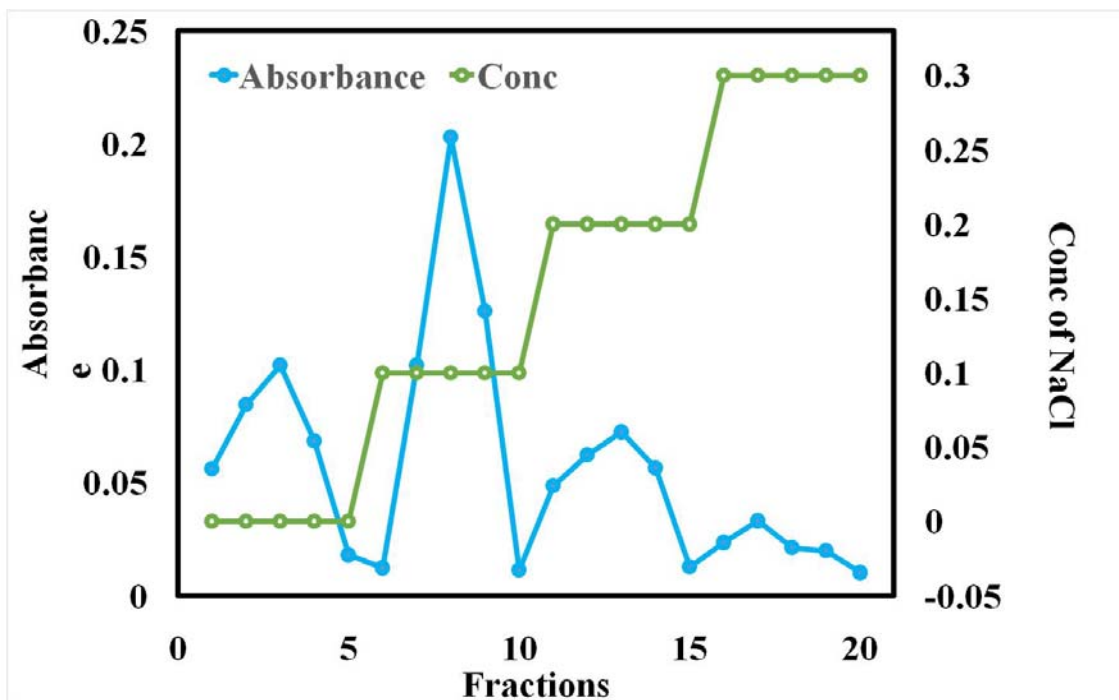


Figure S1. Elution profile of SP-He

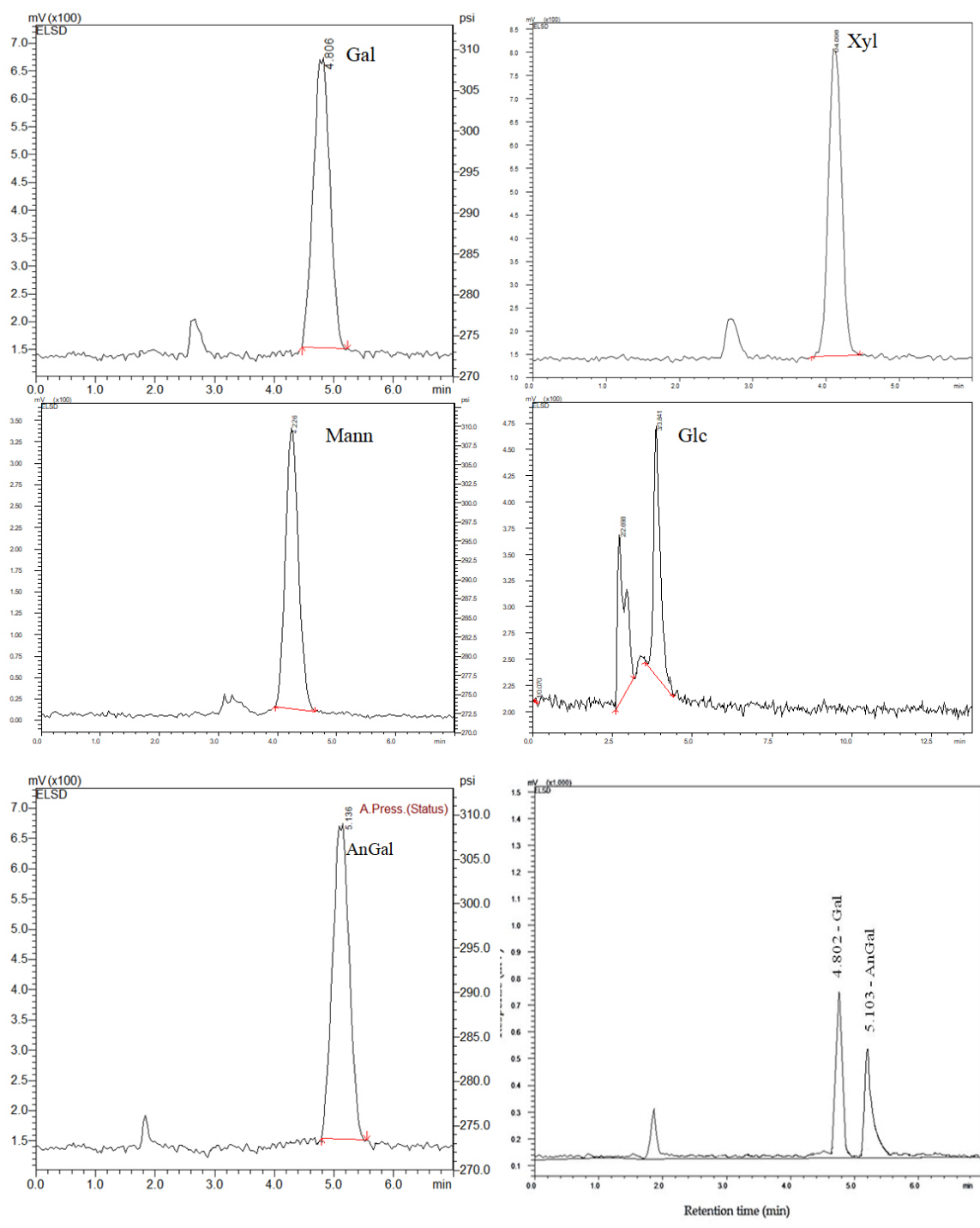


Figure S2. Monosaccharide composition analysis of SP-He-2 and standards

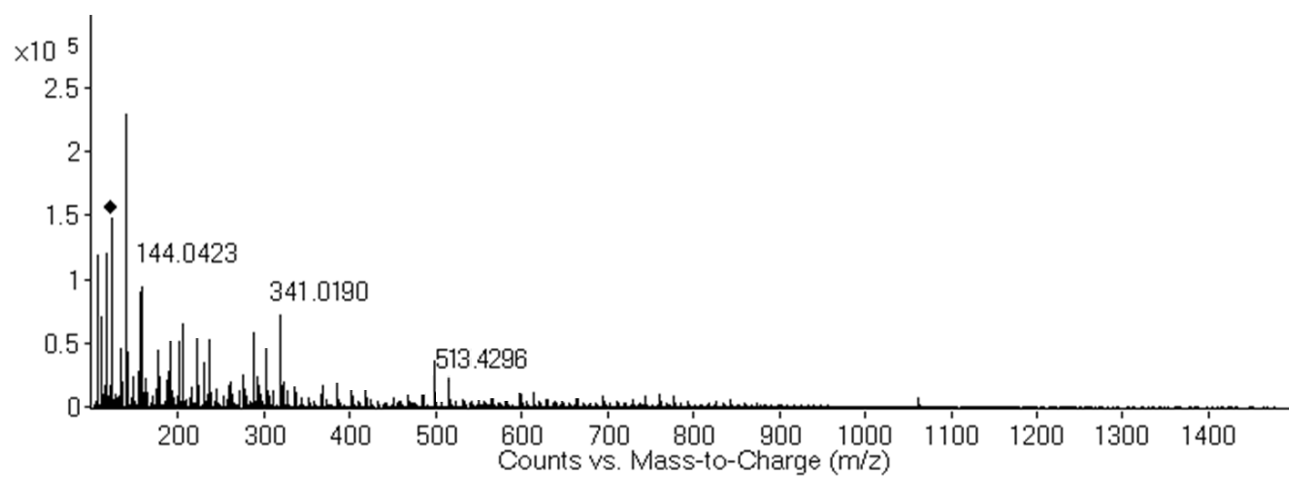


Figure S3. HR-ESIMS spectrum of SP-He-2

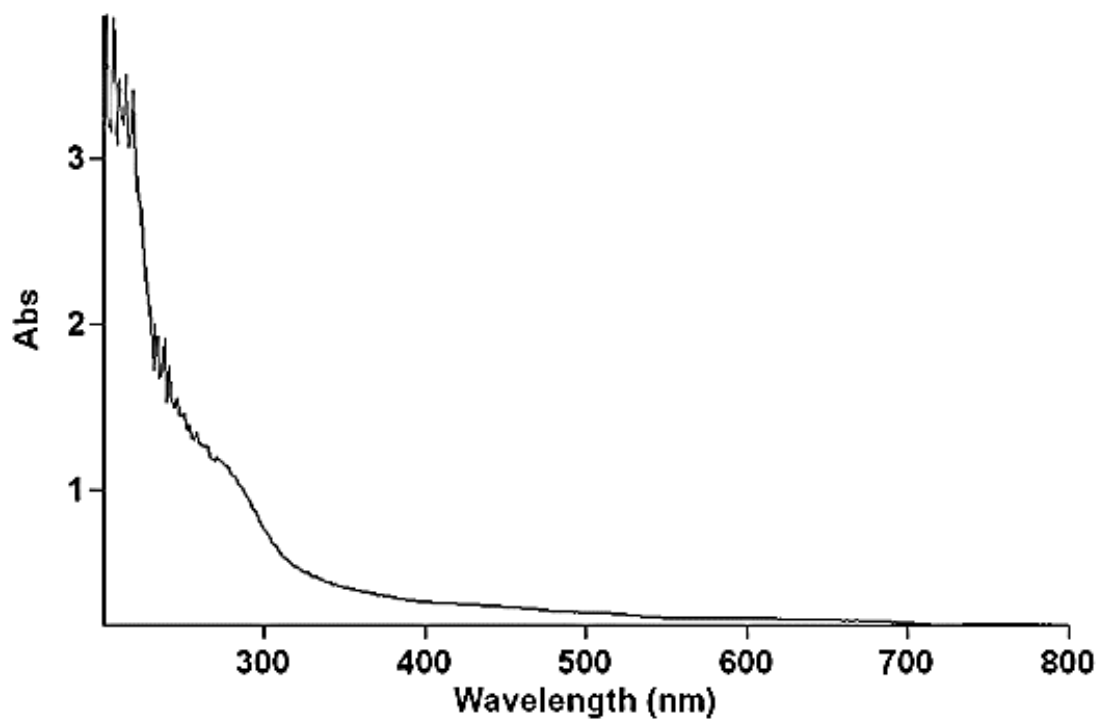


Figure S4. UV-visible spectrum of SP-He-2

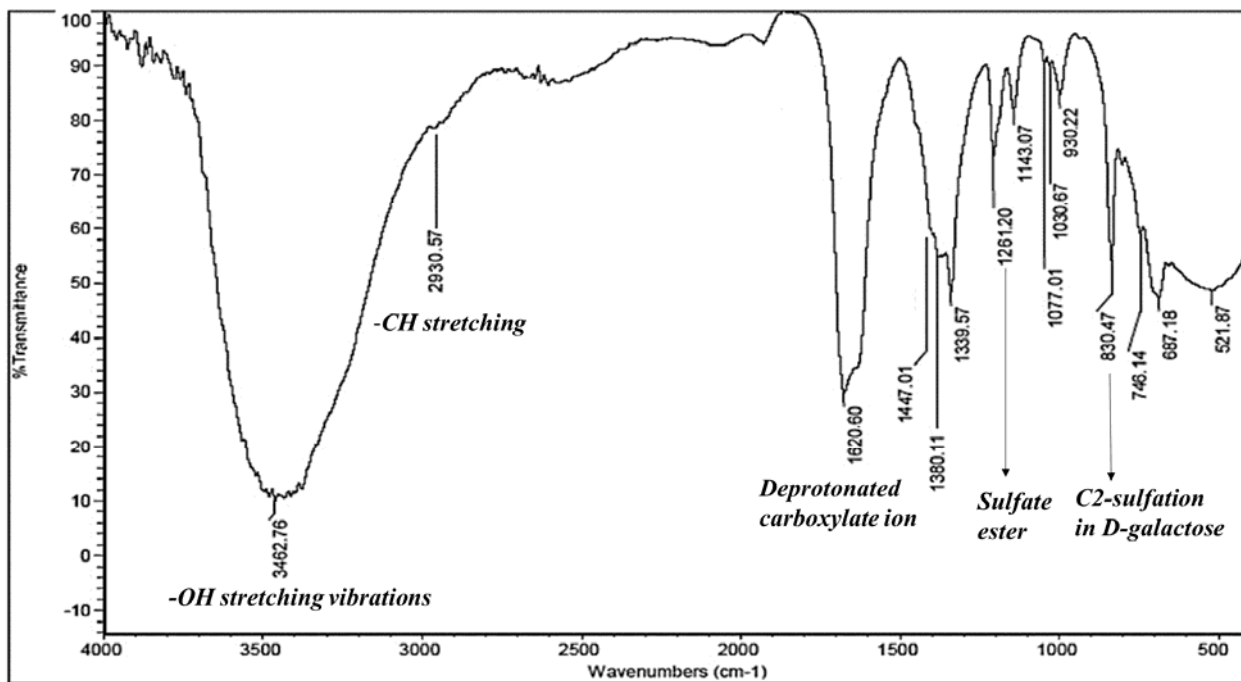


Figure S5. IR spectrum of SP-He-2.

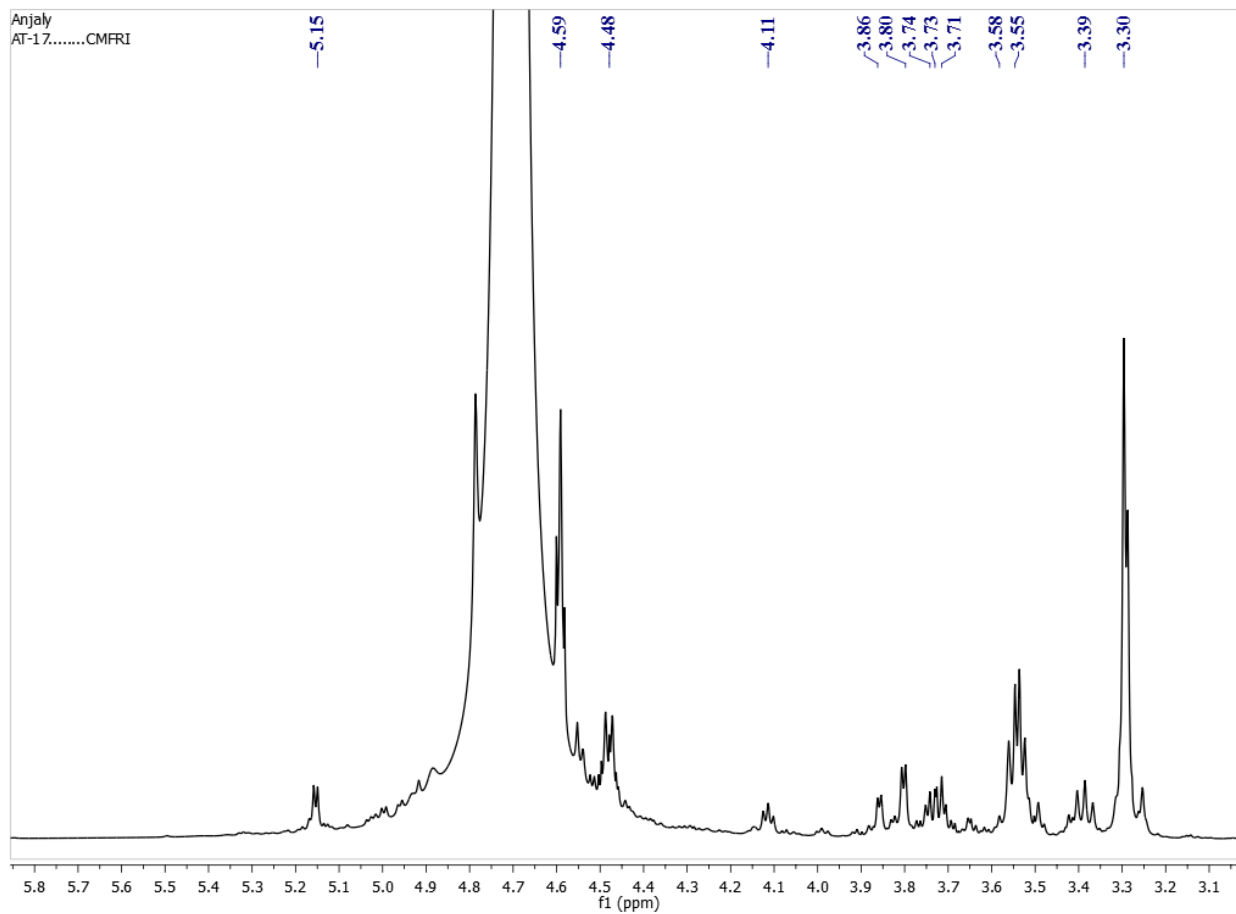


Figure S6. ^1H NMR spectrum of hydrolyzed SP-He-2

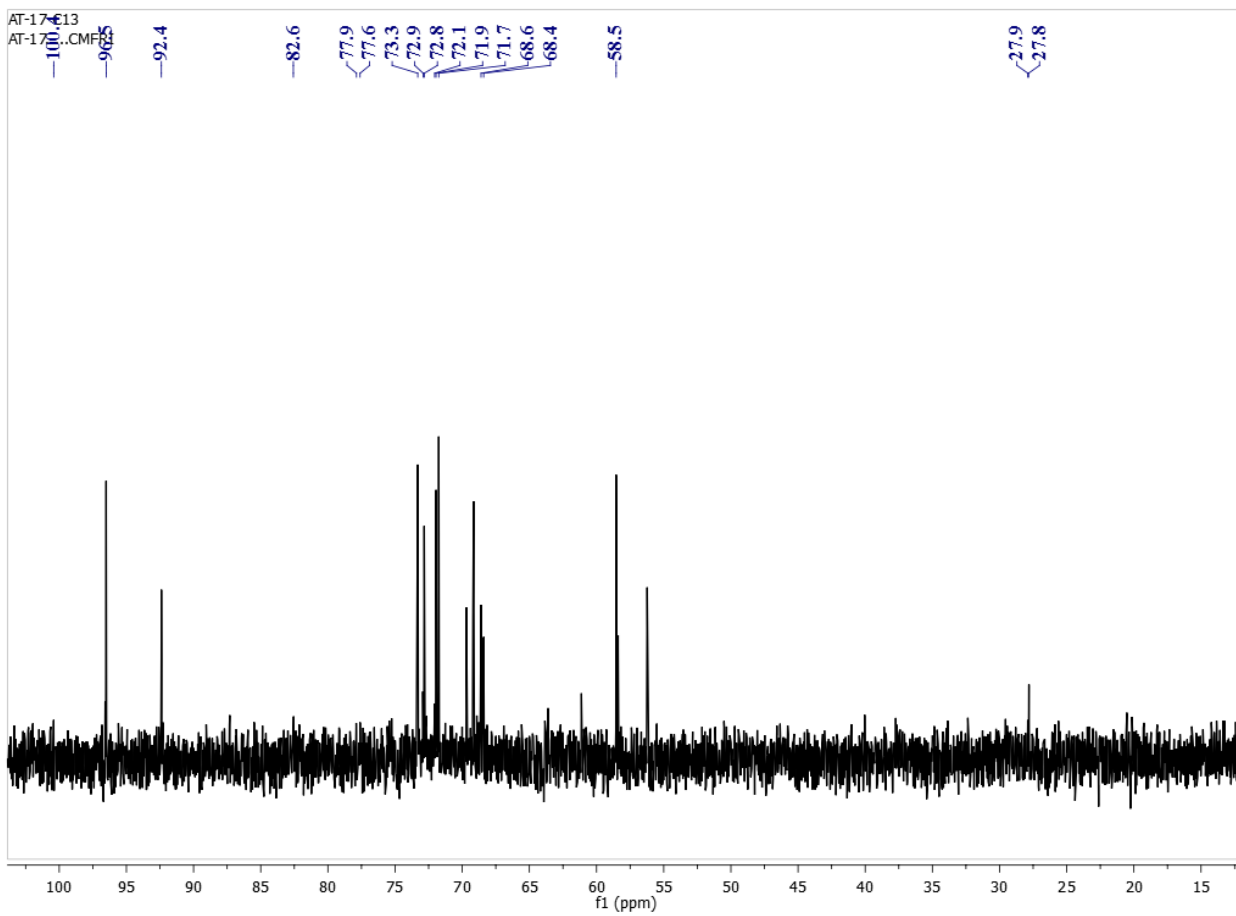


Figure S7. ^{13}C NMR spectrum of hydrolyzed SP-He-2

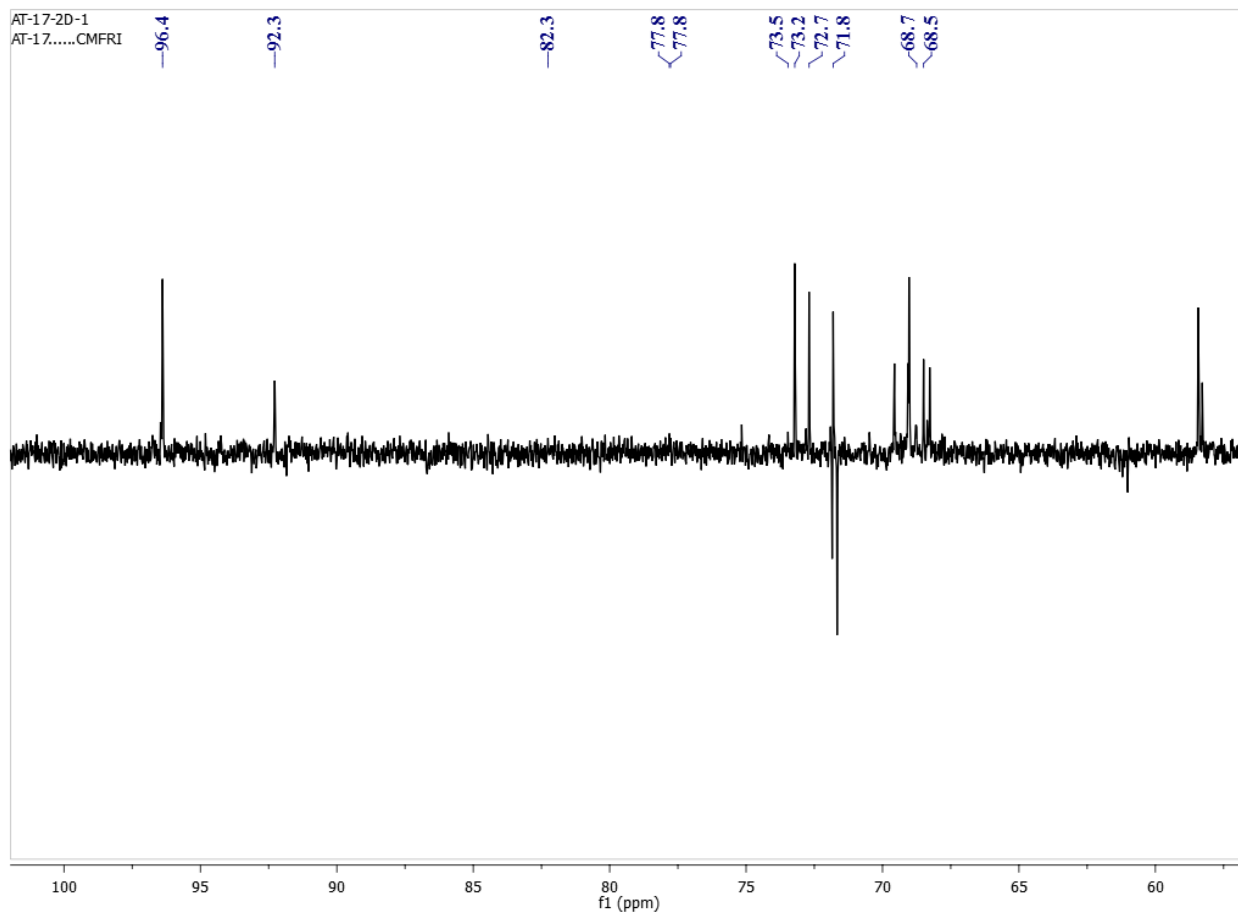


Figure S8. DEPT¹³⁵ spectrum of hydrolyzed SP-He-2

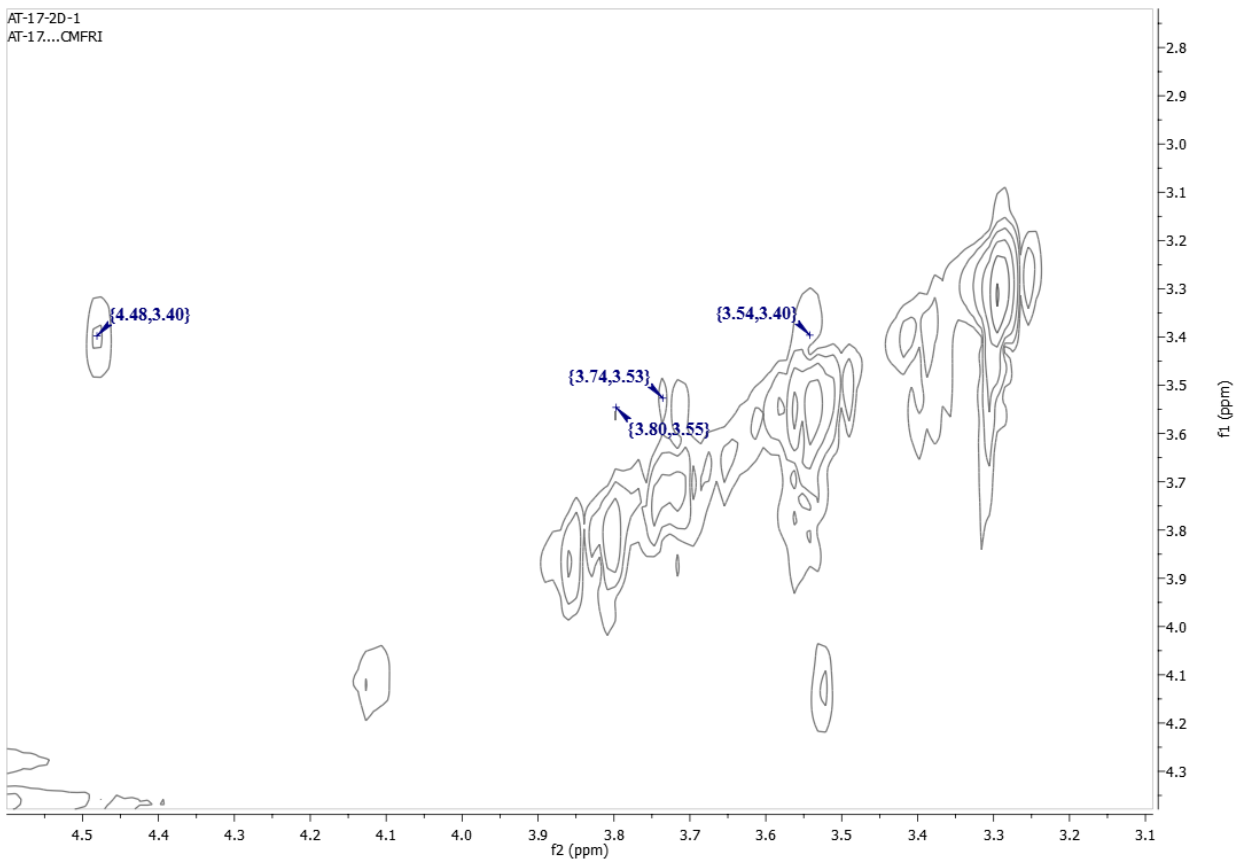


Figure S9. ^1H - ^1H COSY NMR spectrum of hydrolyzed SP-He-2

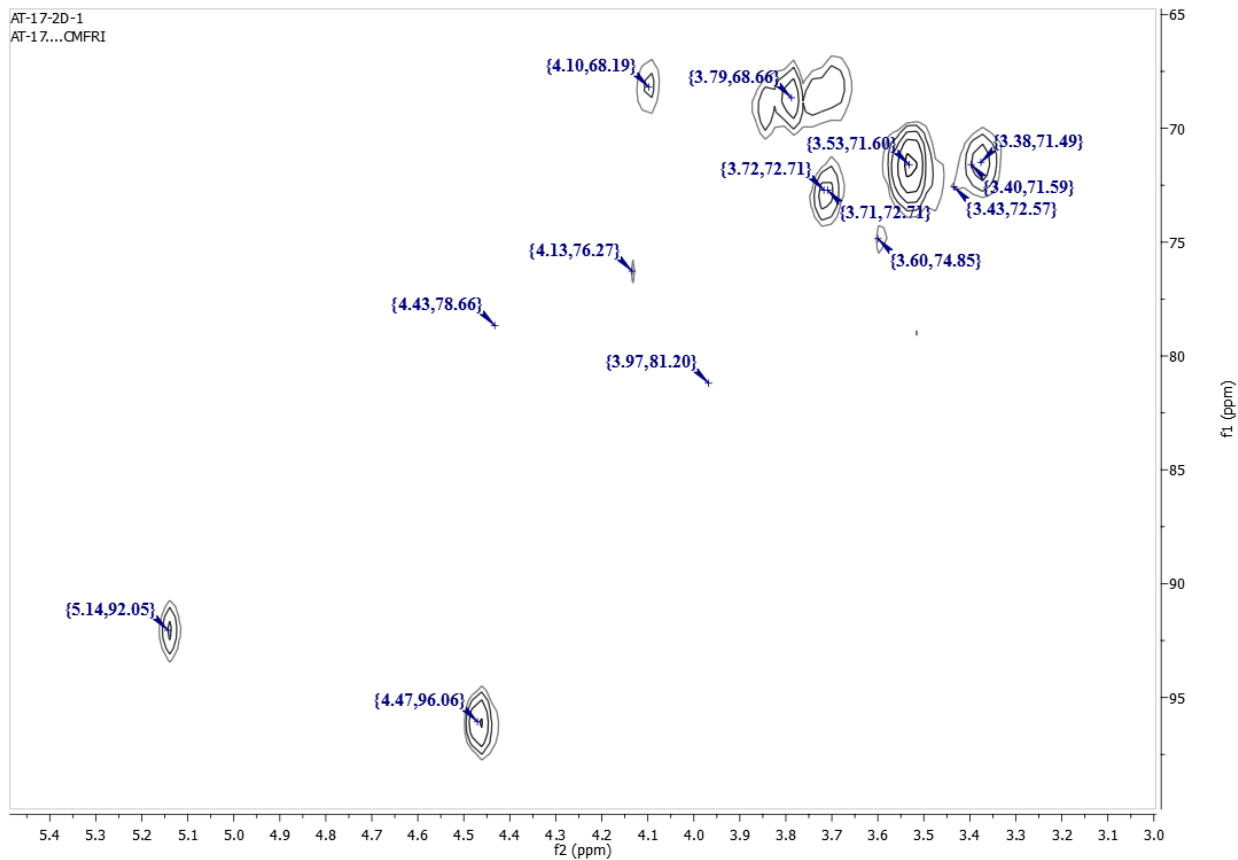


Figure S10. HSQC spectrum of hydrolyzed SP-He-2

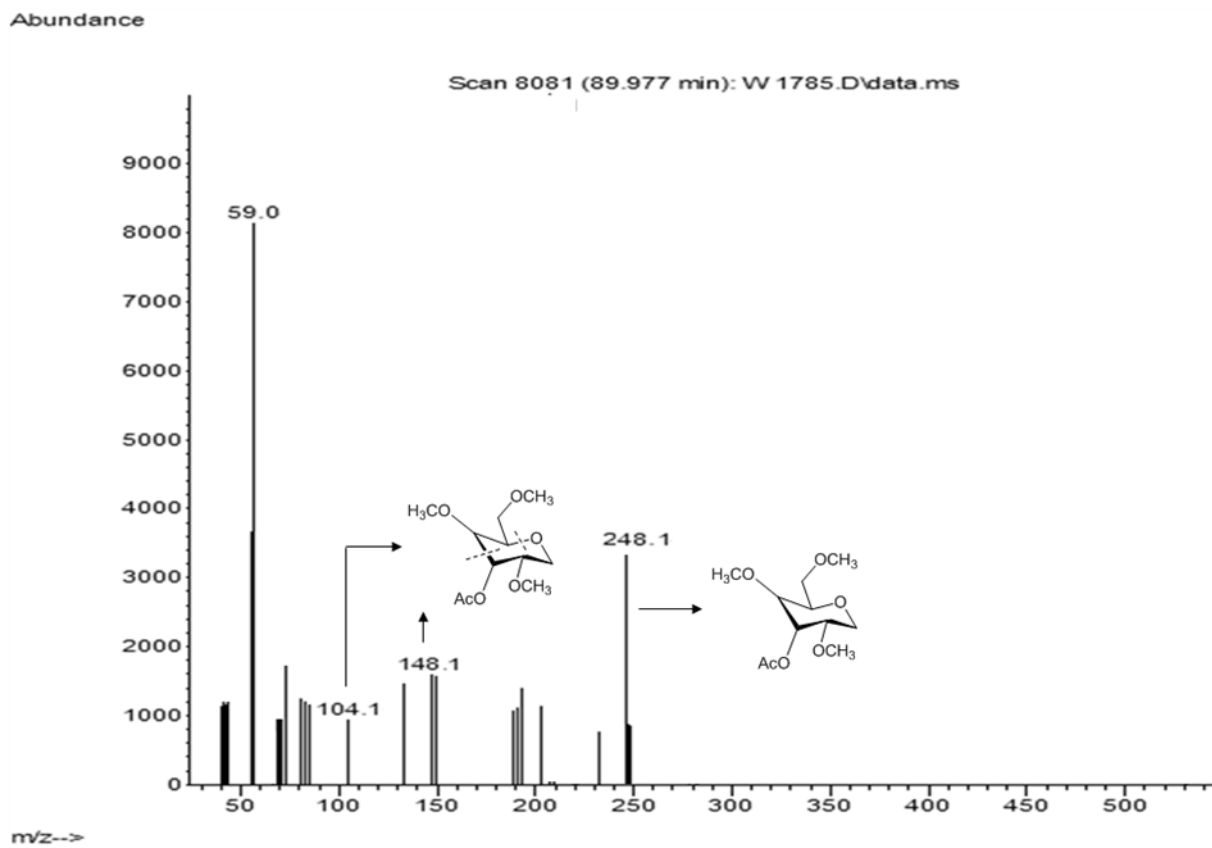


Figure S11. EI-MS spectrum of 3-*O*-acetyl-2,4,6-tri-*O*-methyl galactitol

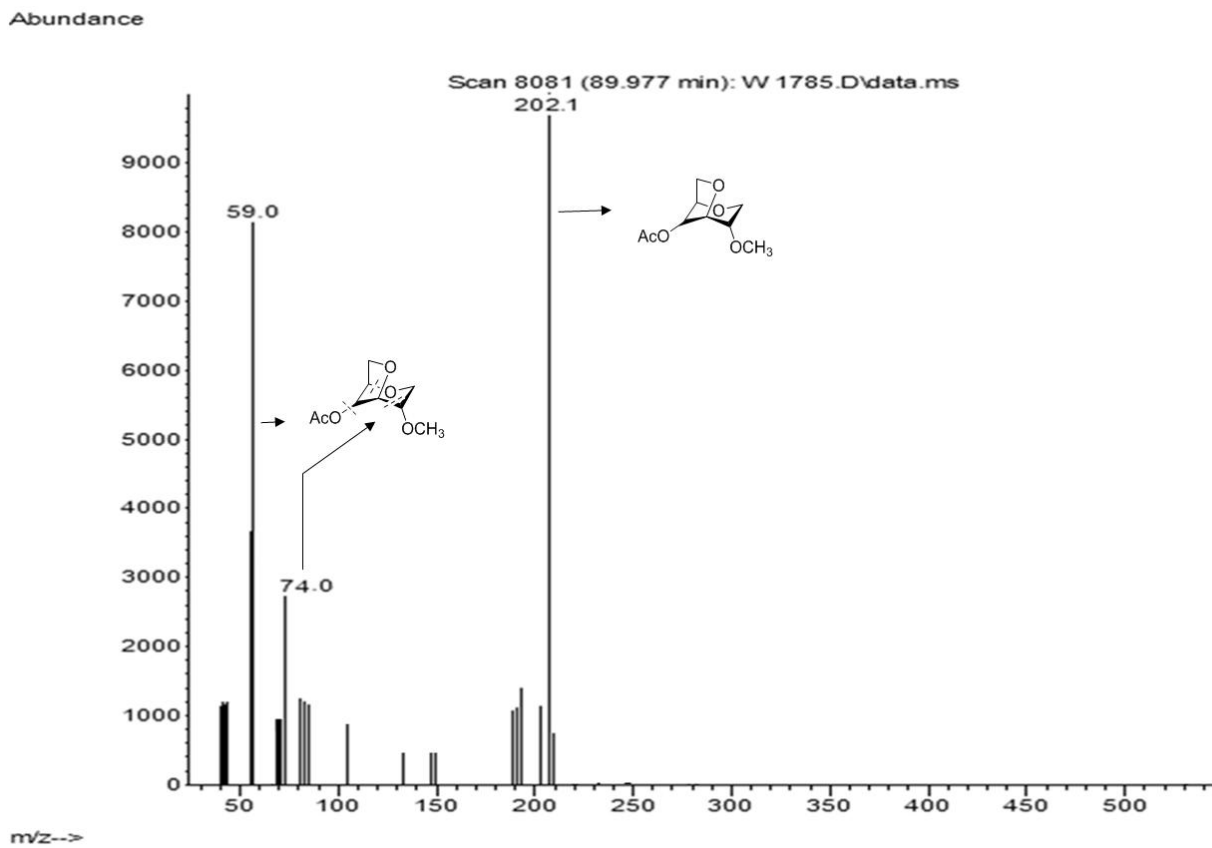


Figure S12. EI-MS spectrum of 4-*O*-acetyl-3,6-anhydro-2-*O*-methyl galacitol

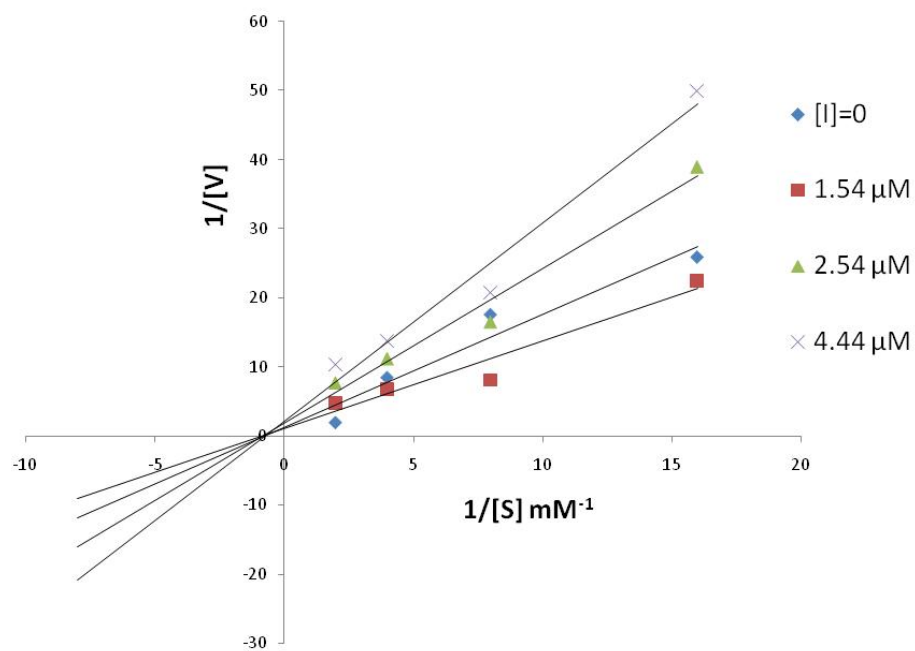


Figure S13. Lineweaver-Burk plots for the inhibition of SP-He-2 on DPP-IV

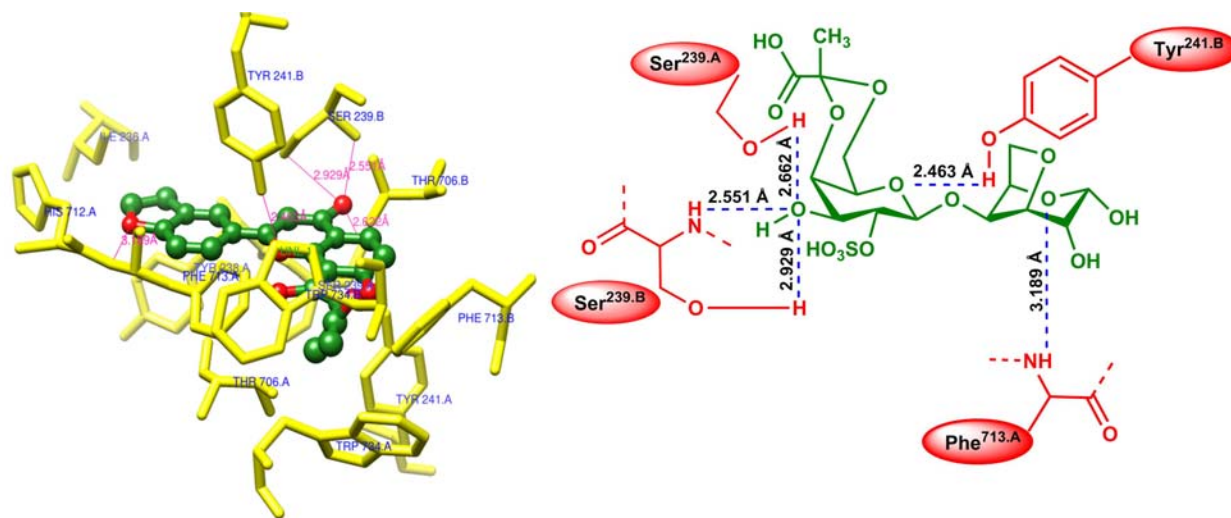


Figure S15. Molecular docking analysis of SP-He-2 and hydrogen bonds of polysaccharide unit